

Bithiazole-bridged dyes for dye-sensitized solar cells with high open circuit voltage performance

Jinxiang He, Wenjun Wu, Jianli Hua,* Yihua Jiang, Sanyin Qu, Jing Li, Yitao Long and He Tian*

Received 7th November 2010, Accepted 9th February 2011

DOI: 10.1039/c0jm03811c

Five new metal-free organic dyes (T1–T5) containing bithiazole moieties were synthesized and used for dye-sensitized solar cells (DSSCs). Their absorption spectra, electrochemical and photovoltaic properties were fully characterized. Electrochemical measurement data indicate that the tuning of the HOMO and LUMO energy levels can be conveniently accomplished by alternating the donor moiety. All of these dyes performed as sensitizers for the DSSC test, and the photovoltaic performance data of these bithiazole-bridged dyes showed higher open circuit voltages (745–810 mV). Among the five dyes, T1 showed the best photovoltaic performance: a maximum monochromatic incident photon-to-current conversion efficiency (IPCE) of 83.8%, a short-circuit photocurrent density (J_{sc}) of 11.78 mA cm⁻², an open-circuit photovoltage (V_{oc}) of 810 mV, and a fill factor (ff) of 0.60, corresponding to an overall conversion efficiency of 5.73% under standard global AM 1.5 solar light condition, which reached 93% with respect to that of an N719-based device fabricated under similar conditions. The result shows that the metal-free dyes based on bithiazole π -conjugation are promising candidates for improvement of the performance of DSSCs.

1. Introduction

Dye-sensitized solar cells (DSSCs) have attracted considerable scientific and industrial interest as a promising candidate for a new renewable energy source during the past decades.¹ DSSCs based on Ru(II)-polypyridyl complexes photosensitizers, such as N3, N719, and the black dye, have achieved record light-to-power conversion efficiencies exceeding 11% under AM 1.5 simulator.² As an economically feasible alternative to conventional inorganic photovoltaic devices, they offer relatively low-cost solar devices with a high solar-energy-to-electricity conversion efficiency.³ However, in recent years enormous studies have been focused on metal-free organic dyes for use in DSSCs due to their high extinction coefficient, facile molecular design, simple synthesis process, low cost, and no concern with the noble metal resource. Recently, novel organic dyes based on porphyrin,⁴ perylene,⁵ cyanine,⁶ xanthenes,⁷ merocyanine,⁸ coumarin,⁹ hemicyanine,¹⁰ indoline,¹¹ diketopyrrolopyrrole¹² and ethylenedioxythiophene,¹³ have been investigated as sensitizers for DSSCs, and great progress has been made in this field.

The open circuit voltage is an important factor for the power conversion efficiency of DSSCs. Charge recombination processes of injected electrons with I₃⁻ ions in the electrolyte¹⁴ and the

oxidized dyes¹⁵ are considered to be responsible for the lowering of the open circuit voltage, which is far below the theoretical maximum.¹⁶ In order to restrain this charge recombination process, double layered TiO₂ electrodes, 4-*tert*-butylpyridine, ruthenium cyclodextrin complexes, and saccharide blocking layers have been used in DSSCs.¹⁷ Recently it was found that bridge groups carrying lateral alkyl chains helped to form a blocking layer to keep I₃⁻ ions away from the TiO₂ electrode surface, hence increasing the electron lifetime and open circuit voltage (V_{oc}).¹⁸

Thiazole is well-known electron-deficient unit because it contains one electron-withdrawing nitrogen of the imine (–C=N) in place of the carbon atom at the 3-position of thiophene.¹⁹ Alkyl chain-substituted bithiazole with two thiazole rings connected together have also been used as acceptor unit to copolymerize with the donor unit of oligothiophene^{20,21} or cyclopentadithiophene,²² and present unique electronic and optical properties. Therefore, bithiazole-based polymers have been widely employed in thin film transistors, photovoltaic cells, and light-emitting diodes applications, in which solar cells based on the bithiazole copolymers show high open circuit voltage and a power conversion efficiency of around 3%,^{22b,23} suggesting that bithiazole-based polymers could be promising photovoltaic donor materials. We consider that the thiazole rings with two long alkyl chains can increase their potential applicability as dye-sensitizers for DSSCs. However, to the best of our knowledge, small molecular dyes containing a bithiazole moiety have not been explored for DSSCs. On the other hand, triarylamine is

Key Laboratory for Advanced Materials and Institute of Fine Chemicals, East China University of Science & Technology, 130 Meilong Road, Shanghai, 200237, P.R. China. E-mail: tianhe@ecust.edu.cn; Fax: +86-21-64252758; Tel: +86-21-64250940; jlhua@ecust.edu.cn; +86-21-64252288; +86-21-64252756

a well-known nonplanar compound which can improve the hole-transporting ability of the materials and prevent the formation of dye aggregates. Recently, triphenylamine-based dyes have been widely used in organic photovoltaic functional materials and have become the focus of intensive research in the field of solar cells.²⁴ Methoxy groups attached to the triphenylamine can enhance the extent of electron delocalization and the ability to donate the electrons of the sensitizer. Also, the introduction of a thiophene moiety was expected to allow red-shift of the spectrum, and broaden the spectral region of absorption. Meanwhile, the phenylethyne spacer is a semirigid conjugated linker which should favor electron injection.²⁵ Based on the above consideration, we have designed and synthesized five new efficient organic bithiazole-bridge sensitizers (**T1–T5** shown in Fig. 1) with triarylamine as the donor, bithiazole as a π -conjugated bridge, and a cyanoacrylic acid moiety acting as the anchoring group. Finally, the five new sensitizers have been applied successfully to the sensitization of nanocrystalline TiO₂-based solar cells and the corresponding photovoltaic properties, electronic and optical properties are also presented.

2. Experimental

2.1 Materials and reagents

Fluorine-doped SnO₂ conducting glass (FTO glass, transmission > 90% in the visible, sheet resistance 15 Ω /square) was obtained from the Geao Science and Educational Co. Ltd. of China. Methoxypropionitrile (MPN), was purchased from Aldrich. Tetra-*n*-butylammonium hexafluorophosphate (TBAPF₆), 4-*tert*-butylpyridine (4-TBP), and lithium iodide were bought from Fluka and iodine, 99.999%, was purchased from Alfa Aesar.

Tetrahydrofuran (THF) was pre-dried over 4 Å molecular sieves and distilled under an argon atmosphere from sodium benzophenone ketyl immediately prior to use. Triethylamine (TEA) and *N,N*-dimethyl formamide (DMF) were heated under reflux with calcium hydride and distilled before used. The starting materials 4-ethynyl-*N,N*-diphenylamine, dimethyl-4-(diphenylamino) phenylboronate, 4-ethynylbenzaldehyde,

dimethyl-4-(bis(4-methoxyphenyl)amino)phenylboronate, 4-formylphenyl-boronic acid and 5,5'-dibromo-4,4'-dihexyl-2,2'-bithiazole were prepared according to published procedures.²⁶ All other solvents and chemicals used in this work were of reagent grade and used without further purification.

2.2 Analytical instruments and measurements

NMR spectra were obtained on a Brücker AM 400 spectrometer. Mass spectra were measured with an HP5989 mass spectrometer. The UV-vis spectra were recorded with a Varian Cary 500 spectrophotometer and fluorescence emission spectra were conducted on a Varian Cary Eclipse fluorescence spectrophotometer. Cyclic voltammograms were performed with a Versastat II electrochemical workstation (Princeton applied research) using a normal three-electrode cell with a Pt working electrode, a Pt wire counter electrode, and a regular calomel reference electrode in saturated KCl solution. The electrochemical impedance spectroscopy (EIS) measurements of all the DSSCs were performed using a Zahner IM6e Impedance Analyzer (ZAHNER-Elektrik GmbH & CoKG, Kronach, Germany). The frequency range is 0.1 Hz–100 kHz. The applied voltage bias is -0.70 V. The magnitude of the alternative signal is 10 mV.

2.3 Synthesis of dyes

5-(5'-Bromo-4,4'-dihexyl-2,2'-bithiazol-5-yl)thiophene-2-carbaldehyde (1). 5,5'-Dibromo-4,4'-dihexyl-2,2'-bithiazole (850 mg, 1.73 mmol), Pd(PPh₃)₄ (200 mg, 0.17 mmol), and K₂CO₃ (1.02 g, 0.01 mol) in 10 mL of THF and 5 mL of H₂O were heated to 45 °C under an argon atmosphere for 30 min. A solution of 5-formylthiophen-2-yl boronic acid (270 mg, 1.73 mmol) in THF (10 mL) was added slowly, and the mixture was refluxed for a further 12 h. After cooling to room temperature, the mixture was extracted with CH₂Cl₂ (3 \times 30 mL). The combined organic layers were washed with water and brine and dried with anhydrous Na₂SO₄. The solvent was evaporated, and the residue was purified by column chromatography on silica gel (PE/CH₂Cl₂ = 3/1–2/1, v/v) to give a yellow solid (154 mg, yield: 15%). ¹H NMR (CDCl₃, 400 MHz), δ : 9.85 (s, 1H), 7.67 (d, J = 4.0 Hz, 1H), 7.21 (d, J = 4.0 Hz, 1H), 2.97 (t, J = 7.6 Hz, 2H), 2.77 (t, J = 7.6 Hz, 2H), 1.81–1.67 (m, 4H), 1.42–1.26 (m, 12H), 0.91–0.89 (m, 6H).

4-(5'-Bromo-4,4'-dihexyl-2,2'-bithiazol-5-yl)-*N,N*-bis(4-methoxyphenyl)aniline (2). The synthesis method resembles that of compound **1**, and the compound was purified by column chromatography on silica gel (PE/CH₂Cl₂ = 4/1–1/2, v/v) to give an orange solid (240 mg, yield: 63.2%). ¹H NMR (CDCl₃, 400 MHz) δ : 7.22 (d, J = 8.4 Hz, 2H), 7.11 (d, J = 8.8 Hz, 4H), 6.92 (d, J = 8.4 Hz, 2H), 6.86 (d, J = 8.8 Hz, 4H), 3.81 (s, 6H), 2.79 (d, J = 6.2 Hz, 2H), 2.75 (d, J = 6.0 Hz, 2H), 1.77–1.68 (m, 4H), 1.35–1.26 (m, 12H), 0.90–0.85 (m, 6H).

4-((5'-Bromo-4,4'-dihexyl-2,2'-bithiazol-5-yl)ethynyl) benzaldehyde (3). To a flask containing Pd(PPh₃)₂Cl₂ (70 mg, 0.1 mmol), CuI (50 mg, 0.26 mmol), PPh₃ (15 mg, 0.057 mmol) and 5,5'-dibromo-4,4'-dihexyl-2,2'-bithiazole (500 mg, 1.02 mmol) was added 4-ethynylbenzaldehyde (102 mg, 0.38 mmol) in TEA (25 mL) under an argon atmosphere. The mixture was stirred at

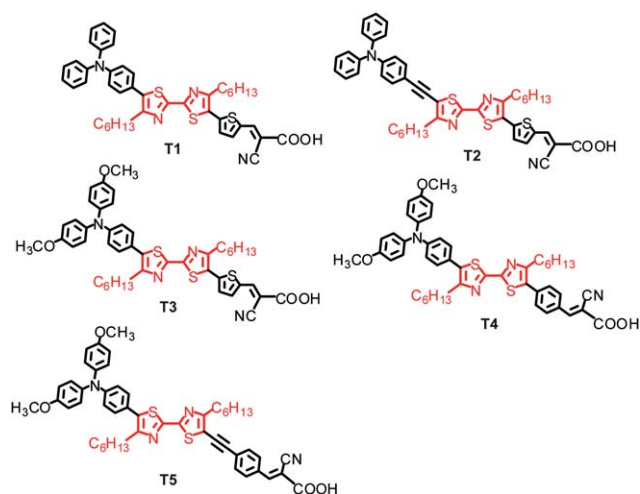


Fig. 1 Molecular structures of bithiazole dyes (**T1–T5**).

reflux for 24 h. The solvent was evaporated, then the residue was diluted with water and extracted with CH₂Cl₂ (3 × 30 mL). The combined organic layers were washed with water and brine and dried with anhydrous Na₂SO₄. The solvent was evaporated, and the remaining crude product was purified by column chromatography using silica gel and CH₂Cl₂/PE (v/v, 1/3–1/2) as the eluent to give a dark yellow solid (160 mg, yield: 23.6%). ¹H NMR (CDCl₃, 400 MHz), δ: 10.04 (s, 1H), 7.89 (d, *J* = 8.4 Hz, 2H), 7.67 (d, *J* = 8.0 Hz, 2H), 2.92 (t, *J* = 7.6 Hz, 2H), 2.77 (t, *J* = 7.6 Hz, 2H), 1.83–1.66 (m, 4H), 1.40–1.25 (m, 12H), 0.92–0.86 (m, 6H).

5-(5'-(4-(Diphenylamino)phenyl)-4,4'-dihexyl-2,2'-bithiazol-5-yl)thiophene-2-carbaldehyde (4). Compound **1** (100 mg, 0.19 mmol), Pd(PPh₃)₄ (22 mg, 0.019 mmol), and K₂CO₃ (1.02 g, 0.01 mol) in 10 mL of THF and 5 mL of H₂O were heated to 45 °C under an argon atmosphere for 30 min. A solution of dimethyl-4-(diphenylamino)phenylboronate (120 mg, 0.38 mmol) in THF (3 mL) was added slowly, and the mixture was refluxed for a further 12 h. After cooling to room temperature, the mixture was extracted with CH₂Cl₂ (3 × 20 mL). The combined organic layers were washed with water and brine and dried with anhydrous Na₂SO₄. The solvent was evaporated, and the residue was purified by column chromatography on silica gel (PE/CH₂Cl₂ = 3/1–2/1, v/v) to give an orange solid (120 mg, yield: 92%). ¹H NMR (CDCl₃, 400 MHz), δ: 9.92 (s, 1H), 7.74 (d, *J* = 4.0 Hz, 1H), 7.32–7.27 (m, 7H), 7.16 (d, *J* = 7.6 Hz, 4H), 7.11–7.06 (m, 4H), 2.99 (t, *J* = 8.0 Hz, 2H), 2.84 (t, *J* = 8.0 Hz, 2H), 1.84–1.72 (m, 4H), 1.38–1.24 (m, 12H), 0.91–0.87 (m, 6H).

5-(5'-((4-(Diphenylamino)phenyl)ethynyl)-4,4'-dihexyl-2,2'-bithiazol-5-yl)thiophene-2-carbaldehyde (5). To a flask containing Pd(PPh₃)₂Cl₂ (70 mg, 0.1 mmol), CuI (50 mg, 0.26 mmol), PPh₃ (15 mg, 0.057 mmol) and compound **1** (200 mg, 0.38 mmol) were added 4-ethynyl-*N,N*-diphenylaniline (102 mg, 0.38 mmol) in TEA (15 mL) and THF (8 mL) under an argon atmosphere. The mixture was stirred at reflux for 24 h. The solvent was evaporated, then the residue was redissolved in CH₂Cl₂ and washed with water and brine. The organic layer was dried with anhydrous Na₂SO₄. The solvent was evaporated, and the remaining crude product was purified by column chromatography using silica gel and CH₂Cl₂/PE (1/3–1/1, v/v) as the eluent gave pure compound **5** as a dark red solid (130 mg, yield: 48%). ¹H NMR (CDCl₃, 400 MHz), δ: 9.92 (s, 1H), 7.74 (d, *J* = 4.0 Hz, 1H), 7.36 (d, *J* = 8.4 Hz, 2H), 7.29 (t, *J* = 7.8 Hz, 4H), 7.27 (d, *J* = 4.0 Hz, 1H), 7.13 (d, *J* = 7.6 Hz, 4H), 7.09 (t, *J* = 7.4 Hz, 2H), 7.02 (d, *J* = 8.8 Hz, 2H), 2.98 (t, *J* = 7.8 Hz, 2H), 2.91 (t, *J* = 7.6 Hz, 2H), 1.82–1.77 (m, 4H), 1.43–1.28 (m, 12H), 0.91–0.86 (m, 6H).

5-(5'-(4-(Bis(4-methoxyphenyl)amino)phenyl)-4,4'-dihexyl-2,2'-bithiazol-5-yl)thiophene-2-carbaldehyde (6). The synthesis method resembles that of compound **1**, and the compound was purified by column chromatography on silica gel (PE/CH₂Cl₂ = 2/1–1/2, v/v) to give a red solid (200 mg, yield: 93%). ¹H NMR (CDCl₃, 400 MHz), δ: 9.91 (s, 1H), 7.73 (d, *J* = 4.0 Hz, 1H), 7.27 (d, *J* = 4.0 Hz, 1H), 7.24 (d, *J* = 8.8 Hz, 2H), 7.12 (d, *J* = 8.8 Hz, 4H), 6.93 (d, *J* = 8.8 Hz, 2H), 6.87 (d, *J* = 8.8 Hz, 4H), 3.81 (s, 6H), 2.99 (t, *J* = 8.0 Hz, 2H), 2.82 (t, *J* = 8.0 Hz, 2H), 1.82–1.74 (m, 4H), 1.43–1.26 (m, 12H), 0.90–0.86 (m, 6H).

4-(5'-(4-(Bis(4-methoxyphenyl)amino)phenyl)-4,4'-dihexyl-2,2'-bithiazol-5-yl)benzaldehyde (7). The synthesis method resembles that of compound **1**, and the compound was purified by column chromatography on silica gel (PE/CH₂Cl₂ = 2/1–1/1, v/v) to give a yellow solid (120 mg, yield: 96.8%). ¹H NMR (CDCl₃, 400 MHz), δ: 10.06 (s, 1H), 7.96 (d, *J* = 8.0 Hz, 2H), 7.64 (d, *J* = 8.4 Hz, 2H), 7.25 (d, *J* = 8.4 Hz, 2H), 7.12 (d, *J* = 8.8 Hz, 4H), 6.94 (d, *J* = 8.8 Hz, 2H), 6.87 (d, *J* = 8.8 Hz, 4H), 3.81 (s, 6H), 2.85 (t, *J* = 5.4 Hz, 2H), 2.81 (t, *J* = 5.4 Hz, 2H), 1.80–1.74 (m, 4H), 1.36–1.28 (m, 12H), 0.89–0.84 (m, 6H).

4-((5'-(4-(Bis(4-methoxyphenyl)amino)phenyl)-4,4'-dihexyl-2,2'-bithiazol-5-yl)ethynyl)benzaldehyde (8). Compound **3** (150 mg, 0.28 mmol), Pd(PPh₃)₄ (32 mg, 0.028 mmol), and K₂CO₃ (1.02 g, 0.01 mol) in 10 mL of THF and 5 mL of H₂O were heated to 45 °C under an argon atmosphere for 30 min. A solution of dimethyl-4-(bis(4-methoxyphenyl)amino)phenylboronate (234 mg, 0.62 mmol) in THF (5 mL) was added slowly, and the mixture was refluxed for a further 12 h. After cooling to room temperature, the mixture was extracted with CH₂Cl₂ (3 × 20 mL). The combined organic layers were washed with water and brine and dried with anhydrous Na₂SO₄. The solvent was evaporated, and the residue was purified by column chromatography on silica gel (PE/CH₂Cl₂ = 2/1–2/1, v/v) to give a red solid (100 mg, yield: 47.2%). ¹H NMR (CDCl₃, 400 MHz), δ: 10.03 (s, 1H), 7.89 (d, *J* = 8.4 Hz, 2H), 7.67 (d, *J* = 8.4 Hz, 2H), 7.24 (d, *J* = 8.4 Hz, 2H), 7.12 (d, *J* = 9.2 Hz, 4H), 6.93 (d, *J* = 8.4 Hz, 2H), 6.87 (d, *J* = 8.8 Hz, 4H), 3.81 (s, 6H), 2.94 (t, *J* = 7.6 Hz, 2H), 2.82 (t, *J* = 7.6 Hz, 2H), 1.83–1.72 (m, 4H), 1.43–1.23 (m, 12H), 0.88 (t, *J* = 6.8 Hz, 6H).

2-Cyano-3-(5-(5'-(4-(diphenylamino)phenyl)-4,4'-dihexyl-2,2'-bithiazol-5-yl)thiophen-2-yl)acrylic acid (T1). Compound **4** (100 mg, 0.14 mmol), 2-cyanoacetic acid (83 mg, 0.98 mmol), ammonium acetate (300 mg) and acetic acid (8 mL) at 120 °C for 12 h. After cooling the solution, water was added to quench the reaction. The precipitate was filtered and washed with water. The residue was purified by column chromatography on silica gel (CH₂Cl₂/EtOH = 20/1, v/v) to yield 133 mg of red solid (yield 82.6%). ¹H NMR (THF-*d*₈, 400 MHz), δ: 8.54 (s, 1H), 8.04 (d, *J* = 4.0 Hz, 1H), 7.62 (d, *J* = 3.2 Hz, 1H), 7.43 (d, *J* = 8.0 Hz, 2H), 7.36 (t, *J* = 8.0 Hz, 4H), 7.15–7.10 (m, 6H), 7.01 (d, *J* = 8.0 Hz, 2H), 2.98 (t, *J* = 7.4 Hz, 2H), 2.80 (t, *J* = 7.4 Hz, 2H), 1.78–1.65 (m, 4H), 1.30–1.23 (m, 12H), 0.85 (t, *J* = 6.8 Hz, 6H). ¹³C NMR (THF-*d*₈, 100 MHz), 165.1, 162.0, 159.0, 158.7, 156.0, 150.6, 149.7, 147.5, 144.2, 140.6, 138.8, 137.6, 132.2, 131.6, 130.2, 128.6, 127.3, 126.9, 125.9, 124.6, 118.1, 117.9, 34.2, 34.0, 33.0, 32.0, 31.9, 31.8, 31.4, 30.4, 29.4, 27.9, 27.8, 24.9, 23.8, 15.8. HRMS (*m/z*): [M + H]⁺ Calcd for C₄₄H₄₅N₄O₂S₃, 757.2705; found, 757.2714. Anal. calcd for C₄₄H₄₄N₄O₂S₃: C 69.81, H 5.86, N 7.40; found C 69.69, H 5.98, N 7.28.

2-Cyano-3-(5-(5'-(4-(diphenylamino)phenyl)ethynyl)-4,4'-dihexyl-2,2'-bithiazol-5-yl)thiophen-2-yl)acrylic acid (T2). A procedure similar to that for the dye **T1** but with compound **5** (120 mg, 0.17 mmol) instead of compound **4** giving the dye **T2** as a dark red solid (95 mg, yield: 72.5%). ¹H NMR (THF-*d*₈, 400 MHz), δ: 8.27 (s, 1H), 7.77 (d, *J* = 4.0 Hz, 1H), 7.33 (d, *J* = 4.0 Hz, 1H), 7.26

(d, $J = 8.8$ Hz, 2H), 7.17 (t, $J = 7.8$ Hz, 4H), 6.99 (t, $J = 7.6$ Hz, 4H), 6.96 (t, $J = 7.4$ Hz, 2H), 6.88 (d, $J = 8.8$ Hz, 2H), 2.87 (t, $J = 7.8$ Hz, 2H), 2.81 (t, $J = 7.6$ Hz, 2H), 1.72–1.65 (m, 4H), 1.34–1.23 (m, 12H), 0.78 (t, $J = 6.8$ Hz, 6H). ^{13}C NMR (THF- d_8 , 100 MHz), 165.1, 164.7, 161.1, 160.2, 158.9, 151.1, 149.6, 149.4, 147.4, 143.7, 140.5, 139.0, 134.6, 131.8, 131.7, 130.4, 129.4, 128.3, 127.9, 127.5, 127.2, 126.9, 126.1, 125.8, 124.4, 123.9, 121.7, 118.6, 117.9, 117.0, 102.5, 102.1, 80.6, 33.9, 33.0, 32.4, 32.0, 31.4, 31.1, 27.2, 27.0, 24.8, 15.8. HRMS (m/z): $[\text{M} + \text{H}]^+$ Calcd for $\text{C}_{46}\text{H}_{45}\text{N}_4\text{O}_2\text{S}_3$, 781.2705; found, 781.2715. Anal. calcd for $\text{C}_{46}\text{H}_{44}\text{N}_4\text{O}_2\text{S}_3$: C 70.74, H 5.68, N 7.17; found C 70.53, H 5.87, N 7.01.

3-(5-(5'-(4-(Bis(4-methoxyphenyl)amino)phenyl)-4,4'-dihexyl-2,2'-bithiazol-5-yl)thiophen-2-yl)-2-cyanoacrylic acid (T3). A procedure similar to that for the dye **T1** but with compound **6** (150 mg, 0.20 mmol) instead of compound **4** giving the dye **T3** as a dark red solid (90 mg, yield: 55.2%). ^1H NMR (THF- d_8 , 400 MHz), δ : 8.38 (s, 1H), 7.91 (d, $J = 3.2$ Hz, 1H), 7.52 (d, $J = 4.0$ Hz, 1H), 7.28 (d, $J = 8.4$ Hz, 2H), 7.10 (d, $J = 8.8$ Hz, 4H), 6.94 (d, $J = 8.8$ Hz, 4H), 6.76 (d, $J = 8.8$ Hz, 2H), 3.75 (s, 6H), 2.94 (t, $J = 7.4$ Hz, 2H), 2.74 (t, $J = 7.4$ Hz, 2H), 1.73–1.64 (m, 4H), 1.30–1.26 (m, 12H), 0.85 (t, $J = 6.6$ Hz, 6H). ^{13}C NMR (THF- d_8 , 100 MHz), 163.5, 161.6, 160.6, 160.5, 158.0, 154.0, 144.4, 140.5, 135.0, 133.7, 132.7, 131.5, 126.2, 123.0, 120.3, 60.5, 38.9, 36.5, 36.2, 35.4, 35.0, 34.2, 34.0, 33.9, 33.8, 33.6, 27.3, 27.2, 19.2, 19.1. HRMS (m/z): $[\text{M} + \text{H}]^+$ Calcd for $\text{C}_{46}\text{H}_{49}\text{N}_4\text{O}_4\text{S}_3$, 817.2916; found, 817.2901. Anal. calcd for $\text{C}_{46}\text{H}_{48}\text{N}_4\text{O}_4\text{S}_3$: C 67.62, H 5.92, N 6.86; found C 67.41, H 6.06, N 5.78.

3-(4-(5'-(4-(Bis(4-methoxyphenyl)amino)phenyl)-4,4'-dihexyl-2,2'-bithiazol-5-yl)phenyl)-2-cyanoacrylic acid (T4). A procedure similar to that for the dye **T1** but with compound **7** (120 mg, 0.16 mmol) instead of compound **4** giving the dye **T4** as yellow solid (110 mg, yield: 84%). ^1H NMR (THF- d_8 , 400 MHz), δ : 8.19 (s, 1H), 7.84 (d, $J = 8.0$ Hz, 2H), 7.34 (d, $J = 8.0$ Hz, 2H), 7.07 (d, $J = 8.0$, 2H), 6.97 (d, $J = 8.8$, 4H), 6.80 (d, $J = 8.0$, 2H), 6.75 (d, $J = 8.8$, 4H), 3.72 (s, 6H), 2.70–2.60 (m, 4H), 1.69–1.57 (m, 4H), 1.27–1.13 (m, 12H), 0.76 (t, $J = 7.2$ Hz, 6H). ^{13}C NMR (THF- d_8 , 100 MHz), 158.8, 155.8, 155.2, 154.1, 147.6, 139.3, 133.9, 131.1, 130.3, 129.9, 128.8, 128.3, 126.0, 121.9, 118.4, 113.8, 54.4, 30.6, 29.1, 28.7, 28.2, 21.6, 13.1. HRMS (m/z): $[\text{M} + \text{H}]^+$ Calcd for $\text{C}_{48}\text{H}_{51}\text{N}_4\text{O}_4\text{S}_2$, 811.3352; found, 811.3346. Anal. calcd for $\text{C}_{48}\text{H}_{50}\text{N}_4\text{O}_4\text{S}_2$: C 71.08, H 6.21, N 6.91; found C 70.98, H 7.07, N 6.73.

3-(4-(5'-(4-(Bis(4-methoxyphenyl)amino)phenyl)-4,4'-dihexyl-2,2'-bithiazol-5-yl)ethynyl)phenyl)-2-cyanoacrylic acid (T5). A procedure similar to that for the dye **T1** but with compound **8** (90 mg, 0.12 mmol) instead of compound **4** giving the dye **T5** as orange solid (93 mg, yield: 95.9%). ^1H NMR (THF- d_8 , 400 MHz), δ : 8.15 (s, 1H), 7.86 (d, $J = 7.8$ Hz, 2H), 7.45 (d, $J = 8.1$ Hz, 2H), 7.11 (d, $J = 8.0$ Hz, 2H), 6.95 (d, $J = 8.8$ Hz, 4H), 6.77 (d, $J = 8.0$ Hz, 2H), 6.75 (d, $J = 8.8$ Hz, 4H), 3.46 (s, 6H), 2.81 (t, $J = 7.2$ Hz, 2H), 2.67 (t, $J = 7.5$ Hz, 2H), 1.73–1.62 (m, 4H), 1.28–1.24 (m, 12H), 0.77 (t, $J = 6.8$ Hz, 6H). ^{13}C NMR (THF- d_8 , 100 MHz), 165.6, 162.6, 159.1, 158.6, 155.4, 151.5, 142.3, 138.0, 135.2, 133.7, 132.7, 131.9, 129.4, 128.0, 124.5, 121.2, 117.0, 116.1, 57.0, 34.0, 33.9, 32.5, 32.0, 31.8, 31.4, 31.2, 31.1, 24.8, 15.8, HRMS (m/z): $[\text{M} + \text{H}]^+$ Calcd for $\text{C}_{50}\text{H}_{51}\text{N}_4\text{O}_4\text{S}_2$, 835.3352; found, 835.3376. Anal. calcd for $\text{C}_{50}\text{H}_{50}\text{N}_4\text{O}_4\text{S}_2$: C 71.91, H 6.03, N 6.71; found C 71.79, H 6.31, N 6.54.

2.4 Device fabrication

A layer of *ca.* 5 μm TiO_2 (13 nm paste, T/SP) was coated on the FTO conducting glass by screen printing and then dried for 6 min at 125 $^\circ\text{C}$. This procedure was repeated 2 times (*ca.* 10 μm) and finally coated by a layer (*ca.* 4 μm) of TiO_2 paste (Ti-nanoxide 300) as the scattering layer. The tri-layer TiO_2 electrodes were gradually heated under an air flow at 275 $^\circ\text{C}$ for 5 min, 325 $^\circ\text{C}$ for 5 min, 375 $^\circ\text{C}$ for 5 min, 450 $^\circ\text{C}$ for 15 min, and 500 $^\circ\text{C}$ for 15 min. The sintered film was further treated with 0.2 M TiCl_4 aqueous solution at room temperature for 12 h, then washed with water and ethanol, and annealed at 450 $^\circ\text{C}$ for 30 min. After the film was cooled to 50 $^\circ\text{C}$, it was immersed in a 3×10^{-4} M dye bath in CH_2Cl_2 solution and maintained in the dark for 12 h at room temperature. The electrode was then rinsed with CH_2Cl_2 and dried. The size of the TiO_2 electrodes used was 0.28 cm^2 . To prepare the counter electrode, the Pt catalyst was deposited on cleaned FTO glass by coating with a drop of H_2PtCl_6 solution (0.02 M 2-propanol solution) with heat treatment at 400 $^\circ\text{C}$ for 15 min. A hole (0.8 mm diameter) was drilled on the counter electrode using a drill-press. The perforated sheet was cleaned with ultrasound in an ethanol bath for 10 min. For the assembly of DSSCs, the dye-covered TiO_2 electrode and Pt-counter electrode were assembled into a sandwich type cell and sealed with a hot-melt gasket of 25 μm thickness made of the ionomer Surlyn 1702 (DuPont). The electrolyte consisting of 0.6 M 1,2-dimethyl-3-propylimidazolium iodide (DMPII), 0.1 M LiI, 0.05 M I_2 , and 0.5 M 4-*tert*-butylpyridine (TBP) in a mixture of acetonitrile and methoxypropionitrile (volume ratio, 7 : 3) was introduced into the cell *via* vacuum backfilling from the hole in the back of the counter electrode. Finally, the hole was sealed using a UV-melt gum and a cover glass.

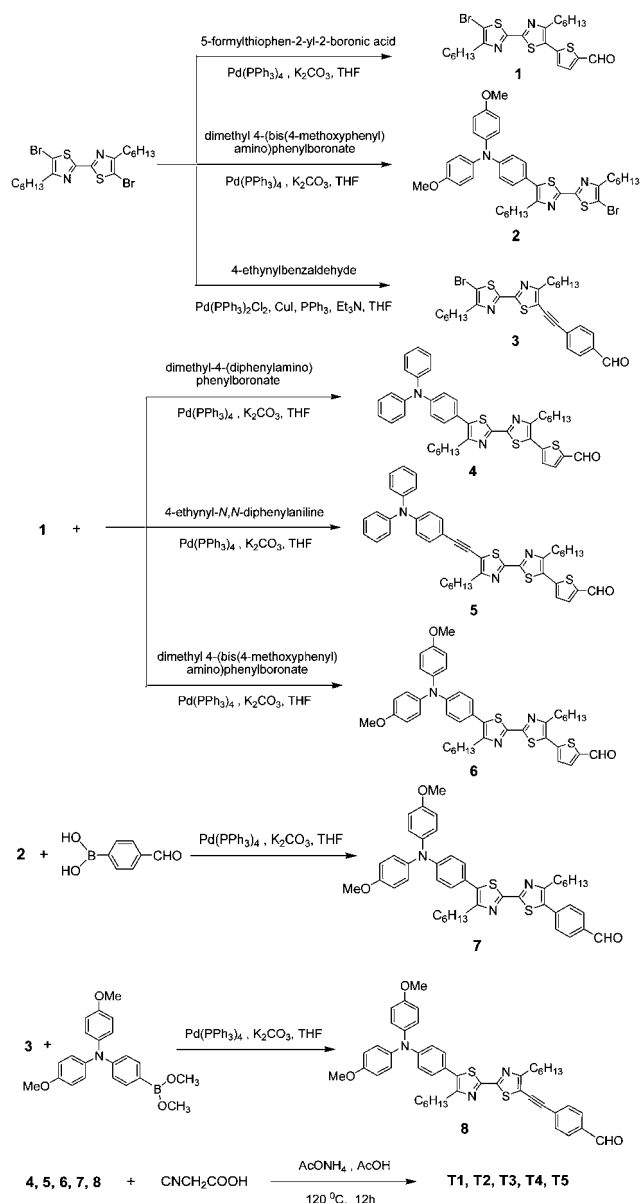
2.5 Photovoltaic properties measurements

Photovoltaic measurements employed an AM 1.5 solar simulator equipped with a 300 W xenon lamp (Model No. 91160, Oriel). The power of the simulated light was calibrated to 100 mWcm^{-2} using a Newport Oriel PV reference cell system (Model 91150V). J - V curves were obtained by applying an external bias to the cell and measuring the generated photocurrent with a Keithley model 2400 digital source meter. The voltage step and delay time of photocurrent were 10 mV and 40 ms, respectively. Cell active area was tested with a mask of 0.196 cm^2 . The photocurrent action spectra were measured with a IPCE test system consisting of a Model SR830 DSP Lock-In Amplifier and a Model SR540 Optical Chopper (Stanford Research Corporation, USA), a 71L/PX150 xenon lamp and power supply, and a 71SW301 Spectrometer.

3. Results and discussion

3.1 Synthesis

The synthetic route to the five dyes (**T1**–**T5**) containing the bithiazole moiety is depicted in Scheme 1. The hexyl chain on the bithiazole group can improve the solubility and form a tightly packed insulating monolayer blocking the I_3^- anions or cations from approaching the TiO_2 . The Suzuki or Sonogashira coupling reaction of 5,5'-dibromo-4,4'-dihexyl-2,2'-bithiazole with 5-



Scheme 1 The synthetic procedure of bithiazole dyes (T1–T5)

formylthiophen-2-yl-2-boronic acid, dimethyl 4-(bis(4-methoxyphenyl)amino)phenylboronate or 4-ethynyl benzaldehyde afforded compounds 1–3, respectively. The reaction produced the di-substituted side products as well, fortunately the monocapped compounds can be easily separated by column chromatography. In the next step, these bromo-exposed intermediates were reacted with dimethyl-4-(diphenyl amino)phenylboronate, 4-ethynyl-*N,N*-diphenylaniline, dimethyl-4-(bis(4-methoxyphenyl)amino)phenylboronate or 4-formylphenylboronic acid by Suzuki or Sonogashira coupling reaction, respectively. Finally, the target products (T1–T5) were synthesized *via* the Knoevenagel condensation reaction of aldehydes 4–8 with cyanoacetic acid in the presence of acetic acid and ammonium acetate. All the key intermediates and five new organic bithiazole sensitizers (T1–T5) were confirmed by ¹H NMR, ¹³C NMR, HRMS and elemental analysis.

3.2 Absorption properties in solution and on the TiO₂ film

Normalized UV-Vis absorption spectra of the dyes (T1–T5) in a diluted solution of CH₂Cl₂ are shown in Fig. 2, and their absorption data are listed in Table 1. All of the dyes (T1–T5) have a relatively broad and strong absorption in the ultraviolet and blue regions with maxima at 457, 465, 460, 410 and 426 nm, respectively. The absorption bands at around 300 nm can be attributed to the π - π^* transition and the bands at around 410–460 nm to the intramolecular charge transfer (ICT) between the donor and the acceptor.^{17,27} T1–T3 were observed to be largely shifted to a longer wavelength than T4–T5 because of the presence of the thiophene instead of the benzene in the π -conjugated linker part. The absorption maximum of T2 at 465 nm was red-shifted by 8 nm relative to that of T1, as T2, containing a triple bond between the triphenylamine and bithiazole, has a larger conjugation length than T1. Compared with T1, T3 has two methoxy groups attached to the triphenylamine on the electron donor side, which enhanced the extent of electron delocalization over the whole molecule, so its maximum absorption peak was red shifted a little. In addition, the absorption maximum of T5 was red-shifted by 16 nm compared with that of T4 due to the introduction of a triple bond between the bithiazole and phenyl moieties. In comparison with conventional ruthenium complexes (for example, $1.39 \times 10^4 \text{ M}^{-1} \text{ cm}^{-1}$ for N719),²⁸ the molar extinction coefficients of the dyes (T1–T5) are obviously larger than that of N719, indicating that these dyes have good light-harvesting ability. The greater maximum absorption coefficients of the organic dyes allows for a correspondingly thinner nano-crystalline film so as to avoid the decrease in the film's mechanical strength. This also benefits the electrolyte diffusion in the film and reduces the recombination possibility of the light-induced charges during transportation.²⁹

The absorption spectra of T1–T5 on TiO₂ films after 3 h adsorption are shown in Fig. 3. The maximum absorption peaks for T1–T5 on the TiO₂ film are at 471, 474, 467, 441 and 448 nm, respectively, in which the absorption bands of the dyes on the TiO₂ films are red-shifted by 14, 9, 7, 31 and 22 nm respectively, compared with the solution spectra. The red shifts of the absorption spectra on TiO₂ of T1–T5 are due to the *J*-aggregation of the dyes on the TiO₂ surface, in which *J*-aggregation can also occur readily because of the presence of carboxyl groups in the molecules. Such broaden and red-shifted absorption has been

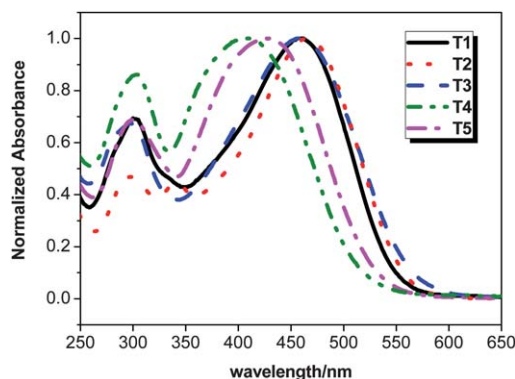
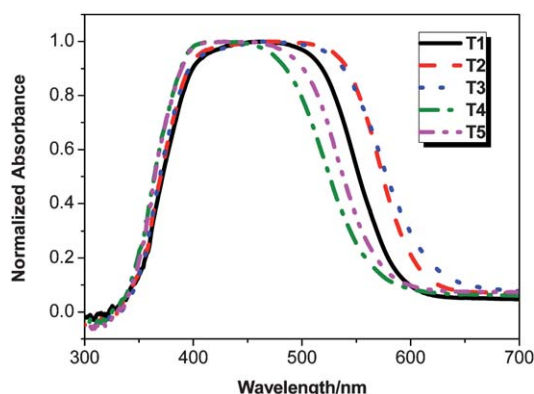


Fig. 2 Normalized absorption spectra of T1–T5 in CH₂Cl₂.

Table 1 Optical and electrochemical properties of bithiazole dyes (**T1–T5**)

Dye	$\lambda_{\max}^a/\text{nm}$ ($\epsilon \times 10^{-4}\text{M cm}$)	$\lambda_{\max}^b/\text{nm}$	HOMO ^c /V (vs. NHE)	E_{0-0}^d/eV	LUMO ^e /V (vs. NHE)
T1	457(3.44)	471	1.06	2.42	-1.36
T2	465(3.93)	474	1.08	2.38	-1.30
T3	460(2.74)	467	0.85	2.37	-1.52
T4	410(1.92)	441	0.84	2.48	-1.64
T5	426(3.12)	448	0.84	2.53	-1.69

^a Absorption maximum in CH_2Cl_2 solution. ^b Absorption maximum on TiO_2 film. ^c HOMOs were measured in THF with 0.1 M tetrabutylammonium hexafluorophosphate (TBAPF₆) as the electrolyte (working electrode: Pt; reference electrode: SCE; calibrated with ferrocene/ferrocenium (Fc/Fc⁺) as an external reference. Counter electrode: Pt wire). ^d E_{0-0} was estimated from the intersection between the absorption and emission spectra. ^e LUMOs are estimated by subtracting E_{0-0} from the HOMO.

**Fig. 3** Normalized absorption spectra of **T1–T5** on TiO_2 film.

reported in other organic sensitizers on TiO_2 electrode due to the *J*-aggregation.^{27b}

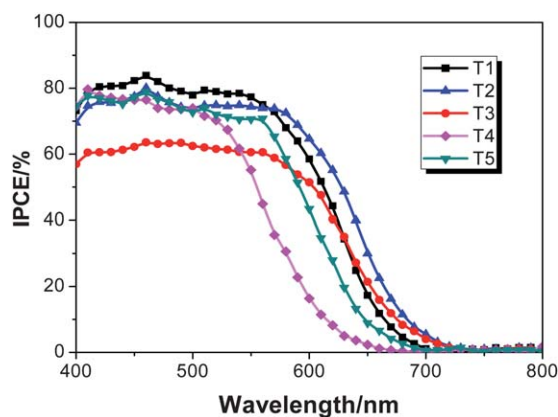
3.3. Electrochemical properties

To evaluate the possibility of electron transfer from the excited dye to the conduction band of TiO_2 , cyclic voltammograms were performed in THF solution using 0.1 M tetrabutylammonium hexafluorophosphate as the supporting electrolyte, Pt as the counter electrode and a saturated calomel electrode (SCE) as reference electrode. The SCE reference electrode was calibrated using a ferrocene/ferrocenium (Fc/Fc⁺) redox couple as an external standard. The highest occupied molecular orbitals (HOMOs) of **T1–T5** corresponding to their first redox potential are 1.06, 1.08, 0.85, 0.84 and 0.84 V vs. NHE, respectively. It is clear that the HOMO levels of **T3–T5** are higher than those of **T1–T2**, which is in agreement with the order of the increase of electron-donating ability of the donors: 4-(bis(4-methoxyphenyl)amino)phenyl > 4-(diphenylamino)phenyl. Generally, the stronger electron-donating ability of the donor resulted in a higher HOMO energy level. The band gap energies ($E_{(0-0)}$) of five the dyes were 2.42, 2.38, 2.37, 2.48 and 2.53 eV for **T1–T5**, respectively, which were estimated from the intercept of the normalized absorption and emission spectra. The estimated excited state potential corresponding to the lowest unoccupied

molecular orbital (LUMO) levels, calculated from $E_{\text{HOMO}} - E_{0-0}$, are -1.36, -1.30, -1.52, -1.64 and -1.69 V, respectively. The examined HOMO and LUMO levels are collected in Table 1. From these data, we found the HOMO levels of **T1–T5** to be sufficiently more positive than the iodine/iodide redox potential value (0.4 V), indicating that the oxidized dyes formed after electron injection into the conduction band of TiO_2 could thermodynamically accept electrons from I^- ions. The LUMO levels of these dyes (see Table 1) were sufficiently more negative than the conduction-band-edge energy level (E_{cb}) of the TiO_2 electrode (-0.5 V vs. NHE), which implies that electron injection from the excited dye into the conduction band of TiO_2 is energetically permitted.³⁰ Noticeably, the relatively large energy gaps between the LUMO levels of the dyes and the conduction band of the TiO_2 semiconductor allow for the addition of the 4-*tert*-butylpyridine (4-TBP) into the electrolyte, which can shift the conduction band of TiO_2 by about -0.3 V and consequently improve the open-circuit voltage and total solar energy conversion efficiency.^{26b}

3.4 Photovoltaic performance of DSSCs

Fig. 4 shows the action spectra of incident photon-to-current conversion efficiency (IPCE) for DSSCs with **T1–T5**. The dye-coated TiO_2 film was used as the working electrode, platinized FTO glass as the counter electrode and 0.6 M DMPII, 0.05 M I_2 , 0.10 M LiI and 0.5 M 4-*tert*-butylpyridine in acetonitrile and methoxypropionitrile (volume ratio, 7 : 3) mixture solution as the redox electrolyte. The losses of light reflection and absorption by the conducting glass were not corrected. As shown in Fig. 4, all five dyes can efficiently convert visible light to photocurrent in the region from 400 nm to 650 nm. The IPCE exceeds 72.5% in the spectral range 400–570 nm for **T1**, which reaches its maximum of 83.8% at 460 nm. The IPCE of **T2–T5** reached a maximum 80.1% at 460 nm, 63.5% at 461 nm, 79.6% at 410 nm and 78.9% at 459 nm, respectively. The IPCE performance of the DSSCs with **T1** is higher than those with **T3–T5** due to its broader photocurrent action spectrum. On the other hand, the IPCE efficiencies of **T1** are higher than that of **T2** in the region from 400 nm to 557 nm, though the IPCE values of **T1** than **T2** are lower in the region 560–700 nm (see Fig. 4), indicating that

**Fig. 4** Photocurrent action spectra of the TiO_2 electrodes sensitized by **T1–T5**.

the **T1** sensitized TiO₂ electrode would generate the highest conversion yield among five dyes.

Fig. 5 shows the current–voltage characteristics of DSSCs fabricated with these thiazole dyes (**T1**–**T5**) as sensitizers under standard global AM 1.5 solar light condition. The detailed parameters of short-circuit current density (J_{sc}), open-circuit voltage (V_{oc}), fill factor (ff), and photovoltaic conversion efficiency (η) are summarized in Table 2. The short circuit current J_{sc} is related to the molar extinction coefficient of the dye molecule, in which a higher molar extinction coefficient have good light-harvesting ability and yields a higher short circuit. **T2** dye has the highest light harvesting efficiency and consequently an improved J_{sc} due to the largest molar extinction coefficient. Compared with **T2**, **T1** has a little lower molar extinction coefficient, but the highest photovoltaic performance among the five dyes. This is probably due to the fact that **T1** has a much higher maximum values of IPCE spectrum than **T2**. Conversely, compared with the **T1** dye, there is dramatic falls in both J_{sc} and V_{oc} values of **T3**, which is ascribed to lower IPCE value of **T3**. The decreased IPCE values suggest that there are inefficient regeneration of the oxidized dye, and accordingly lower J_{sc} (10.97 mA cm⁻²) value is observed. Therefore, it is found that the increase of electron donating ability is not always beneficial to improve the photoelectric conversion efficiency of DSSCs. These results agree well with the corresponding IPCE spectra. In addition, the J_{sc} of **T5** is higher than that of **T4**, this can be attributed to its larger molar extinction coefficient and semirigid conjugated linker of the phenylethyne spacer in **T5** which should favor the electron injection.

As shown in Table 2, it is noteworthy that all of five dyes have higher open circuit voltages (V_{oc}) (745–810 mV) than N719 (672 mV) measured under the same conditions, in which the introduction of two long alkyl chains into the thiazole rings can inhibit the charge recombination and improve V_{oc} . DSSCs based on **T1** exhibit the best overall light to electricity conversion efficiency of 5.73% ($J_{sc} = 11.78$ mA cm⁻², $V_{oc} = 810$ mV, $ff = 0.60$) under AM 1.5 irradiation (100 mW cm⁻²), which reached 93% with respect to that of an N719-based device fabricated under similar conditions. To understand the role of bithiazole-

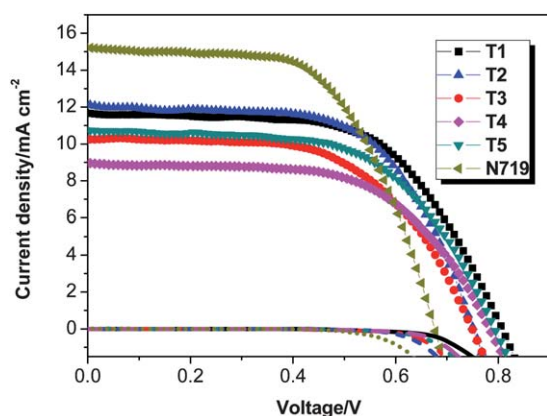


Fig. 5 Photocurrent density vs. voltage curves of DSSCs sensitized by the dyes **T1**–**T5** with electrolyte containing 0.1 M LiI, 0.05 M I₂, 0.6 M DMPII, 0.5 M TBP in the mixed solvent of acetonitrile and 3-methoxypropionitrile (7 : 3, v/v) under light (100 mW cm⁻² simulated AM 1.5 G solar light) and dark.

Table 2 Optical properties and performance parameters of dye-sensitized solar cells of **T1**–**T5**^a

Dye	J_{sc} /mA cm ⁻²	V_{oc} /mV	ff	η (%)
T1	11.78	810	0.60	5.73
T2	12.06	754	0.62	5.60
T3	10.22	745	0.59	4.48
T4	8.92	782	0.60	4.20
T5	10.51	790	0.61	5.05
N719	15.43	672	0.60	6.18

^a Illumination: 100 mW cm⁻² simulated AM 1.5 G solar light; electrolyte containing: 0.1 M LiI + 0.05 M I₂ + 0.6 M DMPII + 0.5 M TBP in the mixed solvent of acetonitrile and 3-methoxypropionitrile (7 : 3, v/v).

bridged dyes in improving V_{oc} . effect of them and N719 on dark current was studied as shown in Fig. 5. It is obvious that the bithiazole-bridged dyes dark current onset potential shifted to a larger value than N719. This dark current change indicates that the introduction of two long alkyl chains into thiazole rings can inhibit charge recombination between injected electrons and I₃⁻ ions in the electrolyte.

3.5. Electrochemical impedance spectroscopy

Electrochemical impedance spectroscopy (EIS) analysis was performed to further clarify the bithiazole-bridged dyes effect on the V_{oc} in DSSCs sensitized by the dyes. Fig. 6 shows the electrochemical impedance spectra for the DSSCs made with TiO₂ electrodes dipped with the five sensitizers (**T1**–**T5**) and N719 in the dark under a forward bias of -0.70 V with a frequency range of 0.1 Hz to 100 kHz. Two semicircles were observed in the Nyquist plots (Fig. 6). The smaller and larger semicircles in the Nyquist plots are attributed to the charge-transfer at the counter electrode and the electron transport at the TiO₂/dye/electrolyte interface, respectively. The radius of the larger semicircle increases in the order **T1** > **T5** > **T4** > **T2** > **T3** > **N719**, indicating that the electron recombination resistance increases from **N719**, **T3**, **T2**, **T4**, **T5** to **T1**^{11b} and is reflected in the improvements seen in the V_{oc} . This result is in agreement with the observed shift in the V_{oc} value under standard global AM 1.5 illumination and dark.

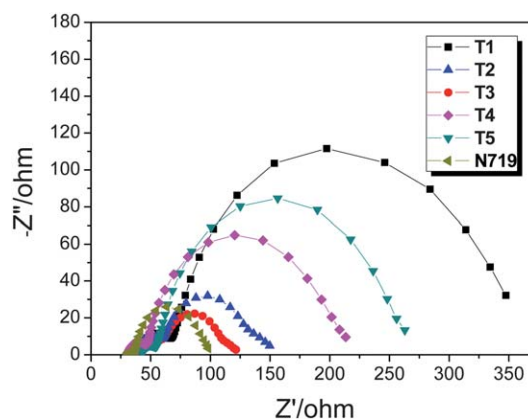


Fig. 6 Impedance spectra of DSSCs based on dye measured at -0.70 V bias in the dark (Nyquist plots).

4. Conclusions

In this paper, five metal-free organic dyes (**T1–T5**) comprising a triarylamine moiety as the electron donor, a cyanoacrylic acid as the anchoring groups, and two hexyl chain substituted bithiazole as the bridge were designed and synthesized for use in dye-sensitized solar cells (DSSCs). The results based on photo-voltaic experiments showed that dyes with two hexyl chain substituted bithiazole unit exhibited a higher open circuit voltage (0.74–0.81V). The power conversion efficiency was shown to be sensitive to the structural modifications of electron donor and bridging linker. Among the five dyes, DSSCs based on **T1** exhibit the best overall light to electricity conversion efficiency of 5.73% ($J_{sc} = 11.78 \text{ mA cm}^{-2}$, $V_{oc} = 810 \text{ mV}$, $ff = 0.60$) under AM 1.5 irradiation (100 mW cm^{-2}). All the results reveal that these metal-free organic bithiazole dyes are promising in the development of DSSCs, and the optimization of their chemical structure and the device is in progress to further improve their energy conversion efficiency.

Acknowledgements

Dedicated to Professor Dao-Ben Zhu on the occasion of his 70th birthday.

This work was supported by NSFC/China (20772031 and 61006048), National Basic Research 973 Program (2011CB808400), the Fundamental Research Funds for the Central Universities (WJ0913001) and Scientific Committee of Shanghai (10520709700).

Notes and references

- (a) B. O'Regan and M. Grätzel, *Nature*, 1991, **353**, 737; (b) A. Hagfeldt and M. Grätzel, *Acc. Chem. Res.*, 2000, **33**, 269; (c) M. Grätzel, *Acc. Chem. Res.*, 2009, **42**, 1788; (d) J.-H. Yum, P. Walter, S. Huber, D. Rentsch, T. Geiger, F. Nüesch, F. D. Angelis, M. Grätzel and M. K. Nazeeruddin, *J. Am. Chem. Soc.*, 2007, **129**, 10320.
- (a) M. Grätzel, *J. Photochem. Photobiol., A*, 2004, **168**, 235; (b) M. K. Nazeeruddin, A. Kay, L. Rodicio, R. Humphry-Baker, E. Müller, P. Liska, N. Vlachopoulos and M. Grätzel, *J. Am. Chem. Soc.*, 1993, **115**, 6382; (c) M. K. Nazeeruddin, P. Péchy, T. Renouard, S. M. Zakeeruddin, R. Humphry-Baker, P. Comte, P. Liska, L. Cevey, E. Costa, V. Shklover, L. Spiccia, G. B. Deacon, C. A. Bignozzi and M. Grätzel, *J. Am. Chem. Soc.*, 2001, **123**, 1613.
- (a) P. Wang, S. M. Zakeeruddin, J. E. Moser, M. K. Nazeeruddin, T. Sekiguchi and M. Grätzel, *Nat. Mater.*, 2003, **2**, 402; (b) D. Shi, N. Pootrakulchote, R. Li, J. Guo, Y. Wang, S. M. Zakeeruddin, M. Grätzel and P. Wang, *J. Phys. Chem. C*, 2008, **112**, 17046.
- (a) T. Bessho, S. M. Zakeeruddin, C.-Y. Yeh, E. W.-G. Diau and M. Grätzel, *Angew. Chem., Int. Ed.*, 2010, **49**, 6646; (b) H. Imahori, Y. Matsuura, H. Iijima, T. Umeyama, Y. Matano, S. Ito, M. Niemi, N. V. Tkachenko and H. Lemmetyinen, *J. Phys. Chem. C*, 2010, **114**, 10656; (c) Y. Lee and C. J. T. Hupp, *Langmuir*, 2010, **26**, 3760.
- (a) T. Edvinsson, C. Li, N. Pschirer, J. Schoeneboom, F. Eickemeyer, R. Sens, G. Boschloo, A. Herrmann, K. Müllen and A. Hagfeldt, *J. Phys. Chem. C*, 2007, **111**, 15137; (b) C. Li, J.-H. Yum, S.-J. Moon, A. Herrmann, F. Eickemeyer, N. G. Pschirer, P. Erk, J. Schoeneboom, K. Müllen, M. Grätzel and M. K. Nazeeruddin, *ChemSusChem*, 2008, **1**, 615; (c) C. Li, Z. Liu, J. Schoeneboom, F. Eickemeyer, N. G. Pschirer, P. Erk, A. Herrmann and K. Müllen, *J. Mater. Chem.*, 2009, **19**, 5405; (d) Y. Jin, J. Hua, W. Wu, X. Ma and F. Meng, *Synth. Met.*, 2008, **158**, 64.
- (a) W. Zhan, W. Wu, J. Hua, Y. Jin, F. Meng and H. Tian, *Tetrahedron Lett.*, 2007, **48**, 2461; (b) X. Ma, J. Hua, Y. Jin, F. Meng, W. Zhan and H. Tian, *Tetrahedron*, 2008, **64**, 345; (c) W. Wu, J. Hua, Y. Jin, W. Zhan and H. Tian, *Photochem. Photobiol. Sci.*, 2008, **7**, 63.
- (a) J. R. Mann, M. K. Gannon, T. C. Fitzgibbons, M. R. Detty and D. F. Watson, *J. Phys. Chem. C*, 2008, **112**, 13057; (b) S. Hattori, T. Hasobe, K. Ohkubo, Y. Urano, N. Umezawa, T. Nagano, Y. Wada, S. Yanagida and S. Fukuzumi, *J. Phys. Chem. B*, 2004, **108**, 15200.
- (a) K. Sayama, K. Hara, N. Mori, M. Satsuki, S. Suga, S. Tsukagoshi, Y. Abe, H. Sugihara and H. Arakawa, *Chem. Commun.*, 2000, 1173; (b) K. Sayama, S. Tsukagoshi, T. Mori, K. Hara, Y. Ohga, A. Shinpo, Y. Abe, S. Suga and H. Arakawa, *Sol. Energy Mater. Sol. Cells*, 2003, **80**, 47.
- (a) K. Hara, K. Sayama, Y. Ohga, A. Shinpo, S. Suga and H. Arakawa, *Chem. Commun.*, 2001, 569; (b) K. Hara, T. Sato, R. Katoh, A. Furube, Y. Ohga, A. Shinpo, S. Suga, K. Sayama, H. Sugihara and H. Arakawa, *J. Phys. Chem. B*, 2003, **107**, 597; (c) K. Hara, Z.-S. Wang, T. Sato, A. Furube, R. Katoh, H. Sugihara, Y. Dan-oh, C. Kasada, A. Shinpo and S. Suga, *J. Phys. Chem. B*, 2005, **109**, 15476; (d) Z. Wang, Y. Cui, K. Hara, Y. Dan-oh, C. Kasada and A. Shinpo, *Adv. Mater.*, 2007, **19**, 1138; (e) Z. Wang, Y. Cui, Y. Dan-oh, C. Kasada, A. Shinpo and K. Hara, *J. Phys. Chem. C*, 2007, **111**, 7224.
- (a) Z. Wang, F. Li and C. Huang, *Chem. Commun.*, 2000, 2063; (b) Y. Chen, C. Li, Z. Zeng, W. Wang, X. Wang and B. Zhang, *J. Mater. Chem.*, 2005, **15**, 1654.
- (a) W. H. Howie, F. Claeysens, H. Miura and L. M. Peter, *J. Am. Chem. Soc.*, 2008, **130**, 1367; (b) D. B. Kuang, S. Uchida, R. Humphry-Baker, S. M. Zakeeruddin and M. Grätzel, *Angew. Chem., Int. Ed.*, 2008, **47**, 1923.
- (a) S. Qu, W. Wu, J. Hua, C. Kong, Y. Long and H. Tian, *J. Phys. Chem. C*, 2010, **114**, 1343; (b) F. Guo, S. Qu, W. Wu, J. Li, W. Ying and J. Hua, *Synth. Met.*, 2010, **160**, 1767.
- W. Zeng, Y. Cao, Y. Bai, Y. Wang, Y. Shi, M. Zhang, F. Wang, C. Pan and P. Wang, *Chem. Mater.*, 2010, **22**, 1915.
- (a) Y. Luo, D. Li and Q. Meng, *Adv. Mater.*, 2009, **21**, 1; (b) D. Li, H. Li, Y. Luo, K. Li, Q. Meng, M. Armand and L. Chen, *Adv. Funct. Mater.*, 2010, **20**, 3358; (c) Z. Ning, Q. Zhang, H. Pei, J. Luan, C. Lu, Y. Cui and H. Tian, *J. Phys. Chem. C*, 2009, **113**, 10307; (d) Z. Ning, Y. Fu and H. Tian, *Energy Environ. Sci.*, 2010, **3**, 1170.
- J. E. Kroeze, N. Hirata, S. Koops, M. K. Nazeeruddin, L. Schmidt-Mende, M. Grätzel and J. R. Durrant, *J. Am. Chem. Soc.*, 2006, **128**, 16376.
- F. D. Angelis, S. Fantacci, A. Selloni, M. Grätzel and M. K. Nazeeruddin, *Nano Lett.*, 2007, **7**, 3189.
- J. Song, F. Zhang, C. Li, W. Liu, B. Li, Y. Huang and Z. Bo, *J. Phys. Chem. C*, 2009, **113**, 13391.
- N. Koumura, Z. Wang, M. Miyashita, Y. Uemura, H. Sekiguchi, Y. Cui, A. Mori, S. Mori and K. Hara, *J. Mater. Chem.*, 2009, **19**, 4829.
- (a) T. Yamamoto, S. Otsuka, K. Namekawa, H. Fukumoto, I. Yamaguchi, T. Fukuda, N. Asakawa, T. Yamanobe, T. Shiono and Z. G. Cai, *Polymer*, 2006, **47**, 6038; (b) M. Mamada, J. I. Nishida, D. Kumaki, S. Tokito and Y. Yamashita, *Chem. Mater.*, 2007, **19**, 5404; (c) G. Sauve and R. D. McCullough, *Adv. Mater.*, 2007, **19**, 1822.
- W.-Y. Wong, X.-Z. Wang, Z. He, K.-K. Chan, A. B. Djurišić, K.-Y. Cheung, C.-T. Yip, A. M.-C. Ng, Y. Y. Xi, C. S. K. Mak and W.-K. Chan, *J. Am. Chem. Soc.*, 2007, **129**, 14372.
- R. P. Kingsborough, D. Waller, R. Gaudiana, D. Mühlbacher, M. Morana, M. Scharber and Z. Zhu, *J. Macromol. Sci., Part A: Pure Appl. Chem.*, 2010, **47**, 478.
- (a) D. H. Kim, B.-L. Lee, H. M. Kang, E. J. Jeong, J. Park, K.-M. Han, S. Lee, B. W. Yoo, B. W. Koo, J. Y. Kim, W. H. Lee, K. Cho, H. A. Becerril and Z. Bao, *J. Am. Chem. Soc.*, 2009, **131**, 6124; (b) K.-C. Li, J.-H. Huang, Y.-C. Hsu, P.-J. Huang, C.-W. Chu, J.-T. Lin, K.-C. Ho, K.-H. Wei and H.-C. Lin, *Macromolecules*, 2009, **42**, 3681.
- (a) F. NarasoWudl, *Macromolecules*, 2008, **41**, 3169; (b) M. Zhang, H. Fan, X. Guo, Y. He, Z. Zhang, J. Min, J. Zhang, G. Zhao, X. Zhan and Y. Li, *Macromolecules*, 2010, **43**, 5706.
- Z. Ning and H. Tian, *Chem. Commun.*, 2009, 5483.
- A. A. Bothner-By, J. Dadok, T. E. Johnson and J. S. Lindsey, *J. Phys. Chem.*, 1996, **100**, 17551.

- 26 (a) C. Suspène, R. Barattin, C. Celle, A. Carella and J.-P. Simonato, *J. Phys. Chem. C*, 2010, **114**, 3924; (b) C. Teng, X. Yang, C. Yang, S. Li, M. Cheng, A. Hagfeldt and L. Sun, *J. Phys. Chem. C*, 2010, **114**, 9101; (c) J. Lee, B.-J. Jung, S. K. Lee, J.-I. Lee, H.-J. Cho and H.-K. Shim, *J. Polym. Sci., Part A: Polym. Chem.*, 2005, **43**, 1845.
- 27 S. Hwang, J. H. Lee, C. Park, H. Lee, C. Kim, C. Park, M. H. Lee, W. Lee, J. Park, K. Kim, N. G. Park and C. Kim, *Chem. Commun.*, 2007, 4887.
- 28 P. Wang, C. Klein, R. Humphry-Baker, S. M. Zakeeruddin and M. Grätzel, *J. Am. Chem. Soc.*, 2005, **127**, 808.
- 29 (a) J. Tang, J. Hua, W. Wu, J. Li, Z. Jin, Y. Long and H. Tian, *Energy Environ. Sci.*, 2010, **3**, 1736; (b) J. Tang, W. Wu, J. Hua, X. Li and H. Tian, *Energy Environ. Sci.*, 2009, **2**, 982.
- 30 (a) R. Z. Li, D. Shi, D. F. Zhou, Y. M. Cheng, G. L. Zhang and P. Wang, *J. Phys. Chem. C*, 2009, **113**, 7469; (b) W. Wu, J. Yang, J. Hua, J. Tang, L. Zhang, Y. Long and H. Tian, *J. Mater. Chem.*, 2010, **20**, 1772.